1482 Russian Chemical Bulletin, International Edition, Vol. 59, No. 8, pp. 1482—1487, August, 2010

The formation of palladium nanocomposite catalysts on the porous silicon used as anodes of fuel cells

N. A. Yashtulov,[a]* S. S. Gavrin,[a] A. A. Revina,[b] and V. R. Flid[a]

[a]*M. V. Lomonosov Moscow State Academy of Fine Chemical Technology,*
86 prosp. Vernadskogo, 119571 Moscow, Russian Federation.
Fax: +7 (495) 434 7111. E-mail: YashtulovNA@rambler.ru
[b]*A. N. Frumkin Institute of Physical Chemistry and Electrochemistry, Russian Academy of Sciences,*
31 Leninsky prosp., 119991 Moscow, Russian Federation.
Fax: +7 (495) 955 4017

Palladium nanoparticles on the porous silicon were synthesized by radiation-chemical reduction in the solution of reversed micelles. The Pd nanoparticles obtained are electron deficient. The porosity, the type of conductivity, the silicon matrix pore geometry, and precursor parameters influence the size, the shape and the charge state of palladium catalysts. The mechanism of H_2 and HCOOH electrooxidation on porous silica in the presence of $Pd^{\delta+}/Pd$ redox pair is proposed.

Key words: palladium nanocomposites, porous silicon, atomic force microscopy, specific adsorption, electrocatalysis.

The unique properties of the porous silicon (PS) offer the possibility for developing electrocatalytic composites with high surface area (more than 400 $m^2 g^{-1}$) and for preparing specific catalysts in the structure directing porous matrix with the desirable size and shape.[1—4] The low-power electric sources of the new generation for electronics compatible with the silicon microchips are constructed on the base of catalytically active PS composites.[5,6] The use of catalysts in the form of nano-sized particles increase their efficiency and decrease their consumption, that is especially important in case of the metals of platinum group. Previously[7,8] we described the results of the synthesis and the application of the palladium, silver and platinum nanocomposite catalysts for the hydrogen-air fuel cells (FC).

The development of FC is considered as one of the main breakthrough technologies in the energetics of the 21st century. The efficiency of the direct transformation of the chemical energy to the electric energy in the cells achieves 50—70%. The fuel in the PS-based FC is hydrogen, methanol, ethanol or formic acid, whereas the oxidant is the oxygen of the air. The reaction products are either H_2O or H_2O with CO_2. In the internal circuit, the ionic electrolyte-conductor should provide migration of ions and separation of the fuel-reductant and the oxidant. In the modern low-temperature FCs the proton exchange membranes are usually utilized as electrolytes. These membranes <0.2 mm thick are prepared from perfluorinated ion-exchange polymer permeable to protons. To increase the efficiency of FC operation the development of catalytically active electrodes reactions on anode and cathode is needed.

In the development of the novel catalytic systems for the low-temperature FC anodes the use of Pd and its composites is at present the most promising option.[2,9] The Pd composites possess high catalytic activity in the reactions of oxidation of the widespread fuel types (hydrogen, formic acid, ethanol, etc.) and they are stable toward CO, which is a common catalyst poison in FCs.[9]

The aim of the present work is the study of influence of conductivity type, porosity, silicon pore geometry and precursor parameters on surface potential, adsorption capacity, charge state, as well as catalytic activity of the synthesized Pd nanoparticles. The search of correlations between the parameters of adsorption composites and their catalytic activity helps one to find the features of the electrochemical reaction mechanisms involving nanocomposite catalysts.

Experimental

The surface potential of PS samples was measured using a NTegra Prima (NT-MDT) atomic-force microscope by probe method of Kelvin.[10] The method of double pass was used: the pattern was determined during the first pass over the studied surface, the electric interaction of the probe with the sample at a fixed distance between the probe and the sample (10 nm) was measured during the second pass. The frequency signal detection

Published in Russian in *Izvestiya Akademii Nauk. Seriya Khimicheskaya,* No. 8, pp. 1450—1455, August, 2010.

allowed the surface potential distribution (U_s) to be traced. The values of U_s for PS at different solubilization extent (ω_0) of palladium solutions were determined on the first stage, the dependencies of U_s of silicon on its porosity at the fixed value of ω_0 of Pd solutions were found on the second stage.

The Pd nanoparticles were synthesized in accordance with the previously described procedure by radiation-chemical reduction of Pd^{2+} ions in anaerobic conditions in reversed micelles solutions with the subsequent adsorption of nanoparticles on the surface of PS.[11,12] The reversed micelles are the micro drops of aqueous solution (pools) stabilized with the surfactant in isooctane. Sodium bis(2-ethylhexyl)sulfosuccinate (AOT) ($C_{20}H_{37}SO_7Na$, 99%, Sigma) was used as a surfactant. The solution of 0.02 *M* $[Pd(NH_3)_4]Cl_2$ complex (chemically pure) was used in the synthesis. The prepared solutions were sealed and then exposed to γ-irradiation ^{60}Co using a PCM-γ-20 setup. The molar water to AOT ratio was varied from 1.5 to 5, that corresponded to the solubilization extent $\omega_0 = [H_2O]/[AOT] = 1.5—5$. The total Pd content in the studied solutions is determined by the value ω_0; for the values ω_0 = 1.5, 3 and 5 the Pd concentrations were $8.1 \cdot 10^{-5}$, $1.62 \cdot 10^{-4}$ and $2.7 \cdot 10^{-4}$ mol L^{-1} respectively. The size and the composition of the nanoparticles formed can be controlled by varying the conditions of synthesis.[2,12] The content of Pd nanoparticles on the surface was varied from 2 to 10 weight % assuming their adsorption in the PS nanopores the surface concentration of Pt lies in the range 6—23 weight %.

The samples of PS n- and p-type conductivity with the different porosity (*P*) (40—78%) were obtained according to the previously described procedures.[7,8] The PS plates were subjected to anode electrochemical etching in water-ethanol solution of HF. During the galvanostatic mode of anodizing the current density was within 20—100 mA cm^{-2}. The resulted width of porous layer was 1 μm, the diameter of pore channels for the PS of n-type was within 20—50 nm, whereas for p-type it was 5—20 nm.

The X-ray photoelectronic spectra of the Pd nanoparticles adsorbed on PS were registered using a Perkin—Elmer PHI 5500 ESCA spectrometer. The monochromatic Al-Kα-emission ($h\nu$ = 1253.6 eV) was used for the activation of photoemission. The spectra with high resolution were obtained with the transmission energy of analyzer equal 29.35 eV and the frequency of data collection equal 0.125 eV per step. The diameter of the analyzed area was 1.1 mm.

The measurements of the adsorption spectra within interval of wavelengths 190—1000 nm were performed using a Shimadzu UV-3101 PC spectrometer at room temperature. The reference solution was 0.15 *M* solution AOT—isooctane.

Results and Discussion

The dependencies of the surface potential of PS and Pd nanocomposites with PS at $\omega_0 = 5$ for n- and p-type of conductivity on the porosity (*P*) of silicon matrix are shown in Fig. 1 and in Table 1. The modification of the plain non-porous (*P* = 0%) silicon with the Pd nanoparticles results in the U_s increase, that suggests the increase in the electronic type conductivity. The pattern of increasing values of U_s is similar for n-type (form 0.6 to 0.99 V) and p-type (from 0.28 to 0.7 V) conductivities. However in the case of adsorption of Pd nanoparticles on the PS an unusual reversed effect is observed. The effect is that not only the values U_s for the Pd-containing composites are lower than for non-porous silicon, but they are also lower than those for PS of any porosity that does not contain Pd. For the Pd nanocomposites with PS of electronic n-type conductivity U_s have approximately the same values as for PS of the hole p-type conductivity in the absence of Pd at the porosity range within 40—80%.

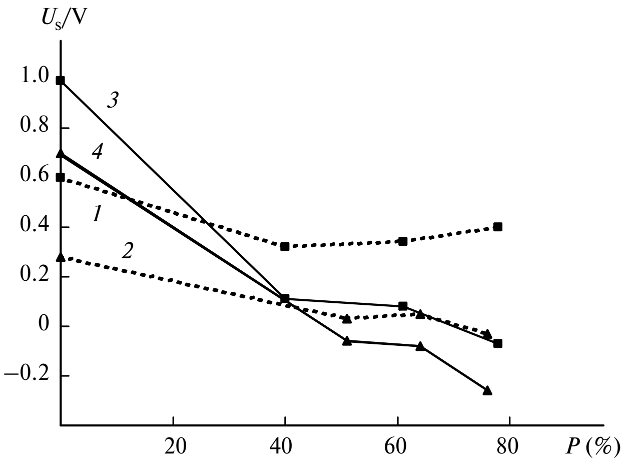

Fig. 1. The dependencies of surface potential of PS (U_s) on the porosity (*P*) at solubilization extent ω_0 = 5 for the samples of PS of n-type (*1*) and p-type (*2*) and for palladium nanocomposites with PS of n-type (*3*) and p-type (*4*).

Table 1. The dependencies of the surface potential of Pd nanocomposites on PS on the porosity level (*P*) of silicon and the type of conductivity at ω_0 = 5

P (%)	Conductivity	U_s(PS)	U_s(Pd + PS)
		V	
0	n	0.60	0.99
0	p	0.28	0.70
40	n	0.32	0.11
51	p	0.03	−0.06
61	n	0.34	0.08
64	p	0.05	−0.08
78	n	0.40	−0.07
76	p	−0.03	−0.26

When the porosity level of pure PS without Pd increases from 40 to 80% the surface potential changes negligibly for silicones of n-type (0.32—0.40 V) and of p-type (from 0.03 to −0.03 V). At the same time, similar to Pd nanocomposites, the decrease of U_s is observed, especially at a porosity level of ~80%. The difference between values of U_s for the nanocomposites of n- and p-type of PS is approximately the same (from 0.16 to 0.19 V) for all samples with $P > 40\%$. It can be thus inferred, that on preparing the active Pd-based electrodes the contribution of both the porosity and the type of conductivity of PS matrix into the summary value of U_s should be taken into consideration. The different behaviour of Pd nanoparticles on the samples of plain and porous silicon, as well as the difference of the U_s values of PS in the absence and in the presence of Pd suggest, that the absorption processes and the charge states of Pd nanoparticles on PS and on the non-porous silicon are different.

The data concerning the influence of the solubilization extent on the changes of the U_s values of Pd nanocomposites on PS of n- and p-type are listed in Table 2. The value ω_0 determines size distribution of Pd nanoparticles in the aqueous pool of the reversed micelles and considerably influences the subsequent formation of nanocomposites in the course of adsorption. It follows from the Table 2, as of the ω_0 value increases the surface potential decreases for nanocomposites with any type of conductivity. The decrease in U_s caused by the increase of ω_0 from 1.5 to 5 for n-type (0.15 V) is nearly the same as that observed for the p-type (0.11 V). The highest U_s change is observed in the solutions with c $\omega_0 = 5$, for which the maximum sizes of the aqueous pool of micelles and an increased content of the small-size fraction of Pd nanoparticles are typical.[2,3]

For the estimation of the charge state and the concentration of the Pd nanocomposites on the PS surface the samples of n- and p-types of conductivity were studied by X-ray photoelectron spectroscopy (XPS) at the fixed value of the porosity and $\omega_0 = 5$. The fragments of high resolution spectra of Pd(3d) with non-linear approximation are shown in Fig. 2. The Pd(3d) spectra consist of duplet $3d_{5/2}$ and $3d_{3/2}$, caused by spin-orbit splitting. In the spectra of the studied samples each of duplet contains two components, corresponding to the two differently charged components of Pd: neutral Pd^0 and ionic Pd^{2+} (see Table 3). In accordance with the reference data[13] the bond energy $E_b(3d_{5/2})$ in Pd metal is 335.1±0.2 eV, whereas for doubly charged ion it is $E_b(3d_{5/2}) = 336.5\pm0.2$ eV. With allowance for the experimental error these values correspond to the peak positions observed for our samples. According to XPS data the contribution of ionic Pd^{2+} state is fairly high and in the samples with PS of n-type it is higher than in case of p-type of surface.

Table 2. The dependence of the surface potential (U_s) of Pd nanocomposites Pd on PS on solubilization extent

The type of conductivity	U_s/V		
	$\omega_0 = 1.5$	$\omega_0 = 3$	$\omega_0 = 5$
n (40)	0.26	0.15	0.11
p (51)	0.05	−0.04	−0.06

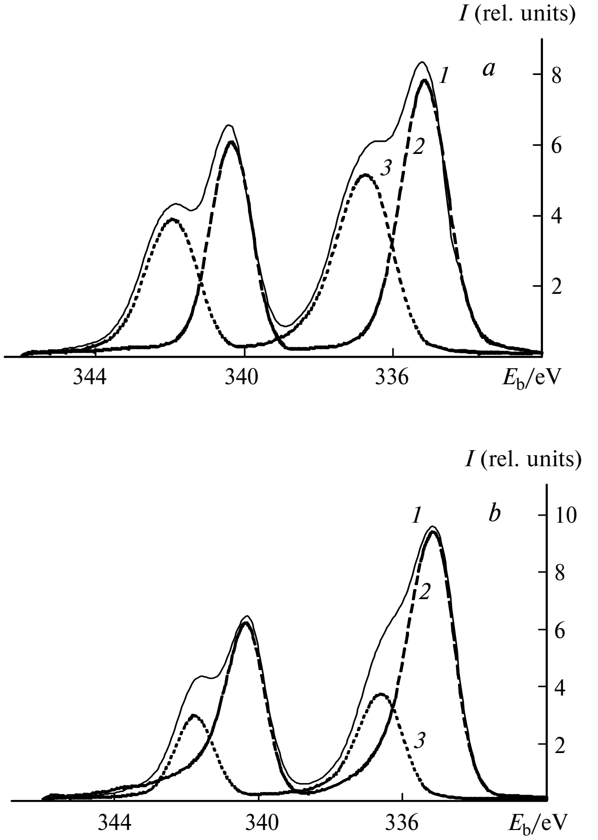

Fig. 2. The XPS spectra of Pd ($3d_{3/2}$ and $3d_{5/2}$) of Pd nanocomposites with PS of n-type (*a*) and p-type (*b*) of conductivity: *1* — general view, *2* — Pd^0, *3* — Pd^{2+}.

Table 3. The characteristics of XPS spectra of Pd nanocomposites on PS with n-type and p-type conductivity

Type of conductivity (*P* (%))	$E_b(3d_{5/2})$/eV		The content of Pd (wt.%)	
	Pd^0	$Pd^{\delta+}$	$Pd^0 + Pd^{\delta+}$	$Pd^{\delta+}/(Pd^0 + Pd^{\delta+})$
n (40)	335.1	336.8	1.6—1.9	40
p (51)	335.1	336.6	6.5—10.3	30

Earlier[11] we analyzed the micro diffraction pictures of the nano-sized Pd particles obtained from the solutions of reversed micelles on the ceramic supports (in particular, silica gel KSK-2) without nanopores. It was shown,[11] that the Pd nanoparticles formed had face-centered cubic lattice with the space group *Fm*3*m*, corresponding to the Pd metal. According to the data of atomic force microscopy (AFM) the nanoparticles of Pd metal were also observed[4,7] on the surface of non porous silica ($P = 0\%$). Therefore, to discuss the catalytic processes on the PS surface one should take into account the contribution of ionic state of palladium nanoparticles $Pd^{\delta+}$, which, probably, can arise as a result of electron density transfer onto the electron deficient PS matrix. The transfer of electronic density from the catalyst onto matrix-carrier was observed earlier[9,14,15,16] for the range of the systems, where the catalyst was in a bulk rather than in the nano-sized state.

The values of the surface potential obtained by AFM, and data on the charge state and the content of nanoparticles obtained by XPS, provide description of the near surface (often monomolecular) layer and not the bulk sample. The Kα-irradiation from Mg and Al used in the present work give the possibility of the collecting the data from the near surface layer with the depth of 2—3 nm or less.

According to the data of XPS the concentrations Pd on the PS surface of n-type and p-type the conductivities are different. The content of the particles adsorbed to the surface of PS of p-type is 3—6 times that of the n-type (see Table 3). These results can suggest the different character of the interaction of Pd nanoparticles with the PS surface of n- and p-type of conductivity.

To specify the adsorption ability of PS of n- and p-type of conductivity the spectrophotometric analysis of reversed micelle palladium solutions in the course of formation of nanocomposites was carried out.

Previously[3,4,7,8,12] by using scanning electron microscopy, AFM, HPLC and spectrophotometry we were able to establish the character of Pd nanoparticles in the liquid phase and on the surface of PS. In the wavelength interval of 190—1000 nm Pd nanoparticles at $\omega_0 = 1.5$, 3 and 5 show two typical bands of plasmon absorption at $\lambda_1 = 230$—265 nm and $\lambda_2 = 290$—320 nm.[3] By comparing the solutions with the different extent of solubilization the hypsochromic shift of the shortwave absorption band ($\lambda = 240$ nm) with the maximal integral intensity can be recognized at $\omega_0 = 5$. Two main fractions of Pd nanoparticles correspond to two bands of plasmon absorption. The particles with small sizes are in the range of 2 to 8 nm, larger particles are 10—14 nm in size. Our data show, that adsorption on PS from the solutions with $\omega_0 = 5$ leads to the formation of spherical nanoclusters with sizes 10 nm or less. In the pools of micellar solutions with $\omega_0 = 3$ the share of large-size fraction (10—14 nm) is the highest. Adsorption on PS the Pd results in ellipsoidal nanoclusters with the lateral sizes ranging from 10 to 40 nm and with the height reaching 8 nm. For the nanoparticles with the lowest sizes of the aqueous pool at $\omega_0 = 1.5$ the shares of small- and large-size fractions are approximately equal. When nanoclusters are formed from these solutions both spherical particles with the sizes lower than 10 nm, and chain structures with the cross section 5—10 nm and the height up to 2 nm appear. This suggests a certain self organization of Pd nanoparticles on the PS surface.[3,4,7,8]

Table 4. The change of the total integral intensity of the absorption of the Pd solutions resulted from the adsorption on PS

Type of conductivity (P (%))	The change of the intensity (%)		
	$\omega_0 = 1.5$	$\omega_0 = 3$	$\omega_0 = 5$
n (40)	22.7	12.7	19.0
p (51)	10.8	6.5	10.9

The results[3] of the measurements of the integral intensity of the characteristic bands of plasmon absorption of Pd nanoparticles ($\lambda_1 = 230$—265 nm, $\lambda_2 = 290$—320 nm), which were obtained during adsorption on the surface of PS of n- and p-type of conductivity within 72 hours, are listed in Table 4. Later on the integral intensity changed insufficiently. The integral intensity is proportional to the number of nanoparticles in the sample and can be a measure of the concentration of the adsorbed palladium nanoparticles. The comparison of the XPS (see Table 3) and spectrophotometry (see Table 4), as well as transmission and scanning microscopy[4,7,8] data shows that Pd nanoparticles are adsorbed both in the near surface PS layer and in the pore volume of silicon matrix. The highest adsorption is observed for the small size (< 10 nm) fractions of nanoparticles ($\omega_0 = 1.5$ and 5) on PS of n-type with the large pores (20—50 nm). For the PS of p-type with the smaller pores (5—20 nm) the adsorption of nanoparticle proceeds mainly on the surface. There can be guest-host relationships between the sizes of precursor nanoparticles and those of the PS nanopores.

Let us try to explain the influence of porosity and solubilization extent on the character of the change of U_s value (see Tables 1, 2 and Fig. 1). The main reason of the decrease in the U_s value is, probably, the partial atomic ionization of Pd nanoparticles, which takes place due to the specific adsorption on the surface in the volume of PS nanopores. As a result of adsorption the formation of electron deficient palladium nanoparticles on PS (Pd$^{\delta+}$/Pd—Si) takes place, that leads to increasing work function of the surface electron and to decrease in U_s. The structural factor of the mutual compatibility of PS nanopores sizes and those of Pd nanoparticles during the formation of nanocomposites is important in the adsorption—ionization cycle. Nanoparticles having dimensions larger than diameters of PS pores cannot enter the pores.

The transfer of electron density from metal-catalyst to electron deficient matrix-carrier is the common phenomenon considered in the practice and the theory of heterogeneous catalysis and is often used for the interpretation of experimental data.[9,14—16]

For example, in a study[14] of features of hydrogenolysis of ethane, propane, cyclopropane, and isobutane it was shown, that the reaction rate is dependent on the value of the induced charge of palladium particles (Pd$^{\delta+}$) during their interaction with the supports (zeolites and SiO$_2$). The study[14] of interactions of methylcyclopentane made it possible to determine that the increase in the reaction rate is caused by the presence of electron deficient Pd$^{\delta+}$

sites. On analysing the mechanism of electrocatalysis of the binary Pd-based systems in the oxidation of hydrogen with CO admixtures, it was found that the rate of H_2 oxidation sharply increases when the large number of electron deficient sites of Pd appear on the surface layer. The features of catalysis of nanocomposites based on Au with Pd, Ni, Co, and Fe immobilized on SiO_2 and Al_2O_3 in the allyl isomerisation of allylbenzene, are explained[15] by appearance of positive charge on Au. The formation of partially charged clusters of $Au^{\delta+}$, active in the isomerization is caused by the shift in electron density from Au to electron deficient sites on the surface. The theoretical evaluation[16] of the mechanism of interaction of Pt nanoparticles with the semi conducting matrix resulted in conclusion, that the appearance of the charges on the Pd/semiconductor boundary is caused by redistribution of electron density, that favors a decrease in the activation energy in electrochemical reactions of oxidation of hydrogen-containing reducing agents.

Let us consider the role of electron deficient $Pd^{\delta+}$ nanoparticles on PS in the electrocatalytic reactions of the main reducing agents for FC. The Pd compounds are used as anodes for FC first of all because palladium is resistant to the presence of CO, which is the main catalytic poison for hydrogen-containing fuels. The formic acid is one of the most promising fuels for micro power electrical sources.[2,6] In the FC with formic acid the anode reaction of the direct oxidation of HCOOH occurs without CO formation (dehydrogenation):

$$\begin{aligned}&\mathrm{HCOOH} \longrightarrow \mathrm{COOH} + \mathrm{H}^+ + \mathrm{e}^- \longrightarrow \\ &\longrightarrow \mathrm{CO_2} + 2\,\mathrm{H}^+ + 2\,\mathrm{e}^-.\end{aligned} \tag{1}$$

The elimination of the side reaction of the indirect oxidation with the CO intermediate formation (dehydratation)

$$\begin{aligned}&\mathrm{HCOOH} \longrightarrow \mathrm{CO_{ads}} + \mathrm{H_2O} \longrightarrow \\ &\longrightarrow \mathrm{CO_2} + 2\,\mathrm{H}^+ + 2\,\mathrm{e}^-\end{aligned} \tag{2}$$

is based on action of the Pd catalyst. The presence of the redox-pair ($Pd^{\delta+}$/Pd—Si), probably, favors catalytic oxidation of CO, which proceeds due to the transfer of electron density to the electron deficient $Pd^{\delta+}$ nanoparticles:

$$\begin{aligned}&\mathrm{Pd}^{\delta+}/\mathrm{Pd{-}Si} + \mathrm{CO} + \mathrm{H_2O} \longrightarrow \\ &\longrightarrow \mathrm{Pd}^{\delta-2}/\mathrm{Pd{-}Si} + \mathrm{CO_2} + 2\,\mathrm{H}^+.\end{aligned} \tag{3}$$

The rate-limiting step of the electrocatalytic hydrogen oxidation on the metals of platinum group is the dissociative homolytic decomposition of the adsorbed H_2 to atoms followed by the step of rapid ionization.[17] However at some conditions the mechanism with the simultaneous hydratation and ionization is possible:

$$(\mathrm{H_2})_{\mathrm{ads}} + \mathrm{H_2O} \longrightarrow \mathrm{H}^{\bullet}{}_{\mathrm{ads}} + \mathrm{H_3O}^+ + \mathrm{e}^-, \tag{4}$$

$$\mathrm{H}^{\bullet}{}_{\mathrm{ads}} + \mathrm{H_2O} \longrightarrow \mathrm{H_3O}^+ + \mathrm{e}^-. \tag{5}$$

In this case the rate-limiting step can be one of the electrochemical steps (4) or (5).[17] The second mechanism includes the heterolytic decomposition with the electrooxidation of H_2 molecule. In the presence of the $Pd^{\delta+}$/Pd—Si redox-pair makes the involvement of heterolytic bond cleavage possible and the acceleration of the electrochemical steps (4) and (5) can also be considered. For example, when $Pd^{\delta+}$ ion is coordinated with H_2 molecule the following interactions occur:

$$\mathrm{Pd}^{\delta+} + (\mathrm{H_2})_{\mathrm{ads}} \longrightarrow [\mathrm{PdH}^{\delta-1}] + \mathrm{H}^+, \tag{6a}$$

$$\begin{aligned}&[\mathrm{PdH}^{\delta-1}] \longrightarrow \mathrm{Pd}^{\delta-1} + \mathrm{H}^{\bullet}{}_{\mathrm{ads}} \longrightarrow \\ &\longrightarrow \mathrm{Pd}^{\delta+} + \mathrm{H}^+ + 2\,\mathrm{e}^-.\end{aligned} \tag{6b}$$

When $Pd^{\delta+}$/Pd pair is coordinated sinchronously with H_2 molecule the following interactions occur

$$\mathrm{Pd{-}Pd}^{\delta+} + \mathrm{H}^-{-}\mathrm{H}^+ \longrightarrow [\mathrm{PdH}^{\delta-1}] + \mathrm{Pd} + \mathrm{H}^+, \tag{7a}$$

$$\begin{aligned}&[\mathrm{PdH}^{\delta-1}] + \mathrm{Pd} + \mathrm{H}^+ \longrightarrow \\ &\longrightarrow \mathrm{Pd{-}Pd}^{\delta+} + 2\,\mathrm{H}^+ + 2\,\mathrm{e}^-.\end{aligned} \tag{7b}$$

The presence of $PdH^{\delta+}$ adducts were determined by means of the low-energy electron diffraction during the study of the mechanism of hydrogen adsorption, while the effect of the substantial increase of the rate of neopentane hydrogenolysis on the zeolite matrix was explained by the formation of $PdH^{\delta+}$ adducts.[14]

Therefore, the results described above showed, that electron deficient palladium nanocomposites form on the surface of PS causing the decrease of the surface potential. The charge state, concentration, size and the shape of palladium nanocomposites are dependent on combination of the structure of nanopores of PS of n- or p-type and the sizes of palladium nanoparticles in the course of adsorption.

The work was financially supported by the Russian Foundation for Basic Research (Projects Nos 09-08-00547 and 09-08-00758).

References

1. H. Lee, S. E. Habas, G. A. Somorjai, P. Yang, *J. Am. Chem. Soc.*, 2008, **130**, 5406.
2. F. L. Chen, M. H. Chang, M. K. Lin, *Electrochim. Acta*, 2007, **52**, 2506.
3. N. A. Yashtulov, S. S. Gavrin, D. A. Tanasyuk, A. A. Revina, *Zh. Neorg. Khim.*, 2010, **55**, 210 [*Russ. J. Inorg. Chem.* (*Engl. Transl.*), 2010, **55**, 180].
4. N. A. Yashtulov, S. S. Gavrin, V. A. Labunov, A. A. Revina, *Nano i mikrosistemnaya tekhnika* [*Nano and Microsystem Technics*], 2008, **8**, 20 (in Russian).
5. G. S. Mishra, S. Sinha, *Catal. Lett.*, 2008, **125**, 139.
6. J. Yeom, G. Z. Mozsgai, B. R. Flachsbart, E. R. Choban, A. Asthana, M. A. Shannon, R. Kenis, *Sens. Actuators B: Chem.*, 2005, **107**, 882.

7. N. A. Yashtulov, S. S. Gavrin, A. A. Ashchekin, D. A. Khoroshilov, *Inzhenernaya Mikroelektronika*, 2008, **124**, 8 [*Chip News* (*Engl. Transl.*), 2008, **1**, 8].
8. N. A. Yashtulov, S. S. Gavrin, *Nanoindustriya* [*Nanoindustry*], 2007, **2**, 36 (in Russian).
9. M. R. Tarasevich, V. A. Bogdanovskaya, B. M. Grafov, N. M. Zagudaeva, K. V. Rybalka, A. V. Kapistin, Yu. A. Kolbanovsky, *Electrokhimia*, 2005, **41**, 840 [*Russ. J. Electrochem.* (*Engl. Transl.*), 2005, **41**, 746].
10. V. L. Mironov, *Osnovy skaniruyushchey elektronnoi mikroskopii* [*The Basics of the Scanning Electron Microspoty*], Tekhnosfera, Moscow, 2004, 144 pp. (in Russian).
11. A. A. Revina, A. N. Kezikov, E. V. Alekseev, E. B. Khaylova, V. V. Volod´ko, *Nanotekhnika* [*Nanotechnics*], 2005, **4**, 105 (in Russian).
12. A. A. Revina, A. N. Kezikov, O. G. Larionov, V. T. Dubenchuk, *Zh. Vsesoyuz. Khim. Obshch. im. D. I. Mendeleeva*, 2006, **4**, 55 [*Mendeleev Chem. J.* (*Engl. Transl.*), 2006, **4**, 55].
13. J. F. Moulder, W. F. Stickle, P. E. Sobol, K. D. Bomben, *Handbook of X-ray Photoelectron Spectroscopy*, Ed. J. Chastain, Perkin—Elmer Corp., Eden Prairie, MN, USA, 1992, 261 pp.
14. O. V. Krylov, *Geterogennyi Kataliz* [*Heterogeneous Catalysis*], Akademkniga, Moscow, 2004, 679 p. (in Russian).
15. S. A. Nikolaev, V. V. Spirin, I. L. Beletskaya, A. Yu. Vasil´kov, A. V. Naumkin, L. A. Tyurina, *Ros. nanotekhnologii* [*Russian Nanotechnologies*], 2007, **2**, 58 (in Russian).
16. *Physico-Chemical Phenomena in Thin Films and Solid Surfaces*, Eds L. I. Trakhtenberg, S. H. Lin, O. J. Ilegbusi, Academic Press, Amsterdam, 2007, **34**, 804 pp.
17. B. B. Damaskin, O. A. Petrii, T. A. Tsyrlina, *Elektrokhimia* [*Electrochemistry*], Khimia, Moscow, 2001, 624 pp. (in Russian).

Received March 10, 2010;
in revised form June 10, 2010